Available online at www.sciencedirect.com
ScienceDirect
Virology 376 (2008) 1 – 12
VIROLOGY
www.elsevier.com/locate/yviro

A zebrafish (*Danio rerio*) model of infectious spleen and kidney necrosis virus (ISKNV) infection

Xiaopeng Xu [a,1], Lichun Zhang [a,1], Shaoping Weng [a], Zhijian Huang [a], Jing Lu [a], Dongming Lan [a], Xuejun Zhong [b], Xiaoqiang Yu [c], Anlong Xu [a,*], Jianguo He [a,*]

[a] *State Key Laboratory of Biocontrol, School of Life Sciences, Sun Yat-sen (Zhongshan) University, Guangzhou, 510275, China*
[b] *Guangzhou Kingmed Center for Clinical Laboratory, Guangzhou, China*
[c] *Division of Cell Biology and Biophysics, School of Biological Science, University of Missouri-Kansas City, Kansas City, USA*

Received 5 August 2007; returned to author for revision 15 November 2007; accepted 14 December 2007
Available online 21 April 2008

Abstract

Zebrafish is a model animal for studies of genetics, development, toxicology, oncology, and immunology. In this study, infectious spleen and kidney necrosis virus (ISKNV) was used to establish an infection in zebrafish, and the experimental conditions were established and characterized. Mortality of adult zebrafish infected with ISKNV by intraperitoneal (i.p.) injection exceeded 60%. ISKNV can be passed stably in zebrafish for over ten passages. The ailing zebrafish displayed petechial hemorrhaging and scale protrusion. Histological analysis of moribund fish revealed necrosis of tissue and enlarged cells in kidney and spleen. The real-time RT-PCR analysis of mRNA level confirmed that ISKNV was replicated in zebrafish. Immunohistochemistry and immunofluorescence analyses further confirmed the presence of ISKNV-infected cells in almost all organs of the infected fish. Electron microscope analyses showed that the ISKNV particle was present in the infected tissues. The establishment of zebrafish infection model of ISKNV can offer a valuable tool for studying the interactions between ISKNV and its host.

Keywords: ISKNV; Zebrafish; Infection model; Immunohistochemistry; Immunofluorescence; Electron microscope

Introduction

Zebrafish (*Danio rerio*) is an inexpensive vertebrate model for studies in genetics, development, toxicology, oncology and apoptosis, and has recently been recognized as a valuable model for immunological studies (Trede et al., 2004). Zebrafish have innate and adaptive immune systems, as well as evolutionarily conserved host defense strategies more similar to those in mammals than in non-mammalian model organisms, such as *Drosophila melanogaster* and *Caenorhabditis elegans* (Pukatzki et al., 2002; Aballay et al., 2000). Mammals and zebrafish have almost all equivalent immune cells and immune effector molecules such as cytokines, complement, and the important innate immune defense strategies like the interferon (IFN)-mediated antiviral response (Altmann et al., 2003, 2004) and Toll-like receptors (TLRs) pathways (Jault et al., 2004; Meijer et al., 2004; Phelan et al., 2005a). The identification of the immunoglobulin Z gene (Danilova et al., 2005) and the novel immune-type receptors (NITRs) (Yoder et al., 2004), as well as the recent discovery of more interleukins (Gunimaladevi et al., 2006; Zhang et al., 2005; Igawa et al., 2006) in zebrafish will lead to a better understanding of the zebrafish immune system. Well-developed adaptive and innate immune systems make zebrafish an ideal model for the study of infectious disease (Van der Sar et al., 2004). In fact, there are many kinds of viral pathogens in water (Suttle, 2005) and zebrafish provide a good tool to study the interaction between host and pathogens.

The infection models for gram-negative bacteria, such as *Salmonella typhimurium* (Van der Sar et al., 2003), *S. arizonae* (Davis et al., 2002), *Vibrio anguillarum* (O'Toole et al., 2004),

* Corresponding authors. J. He is to be contacted at fax: +86 20 84113819. A. Xu, fax: +86 20 84038377.
E-mail addresses: lssxal@mail.sysu.edu.cn (A. Xu), lsshjg@mail.sysu.edu.cn (J. He).
[1] These authors contributed equally to this work.

0042-6822/$ - see front matter © 2007 Elsevier Inc. All rights reserved.
doi:10.1016/j.virol.2007.12.026

and Gram-positive bacteria, such as *Bacillus subtilis* (Herbomel et al., 1999), *Listeria monocytogenes* (Menudier et al., 1996), *Streptococcus iniae*, *S. pyogenes* (Neely et al., 2002, Brenot et al., 2004), and *Mycobacterium marinum* (Prouty et al., 2003) have been identified and well established in zebrafish. Some groups have successfully identified a few viral pathogens that can infect and cause diseases in zebrafish. LaPatra et al. (2000) reported that infectious hematopoietic necrosis virus (IHNV) and infectious pancreatic necrosis virus (IPNV) are able to replicate in adult zebrafish. Sanders et al. (2003) described the susceptibility of adult zebrafish to experimental infection by spring viremia of carp virus (SVCV), and Phelan et al. (2005b) reported that *Snakehead rhabdovirus* (SHRV) can infect both the adult and the embryo of zebrafish. Novoa et al. (2006) demonstrated that expressions of TLR3, IFN alpha and beta, Mx, IFN gamma and TNF alpha are increased at 72 h post-infection with viral haemorrhagic septicemia virus (VHSV) in zebrafish, making zebrafish a good model to evaluate the fish vaccine against VHSV.

Iridoviruses are icosahedral cytoplasmic DNA viruses that infect invertebrates and poikilothermic vertebrates, including insects, fish, amphibians, and reptiles (Williams, 1996). The viral genomes are circularly permuted and terminally redundant, both of which are unique features for a eukaryotic virus (Darai et al., 1983, 1985; Delius et al., 1984; Tidona and Darai, 1997). Additionally, the iridoviruses that infect vertebrates have highly methylated genomes (Darai et al., 1983; Willis and Granoff, 1980). Based on the Eighth Report of the International Committee on Taxonomy of Virus (ICTV), the family Iridoviridae has been subdivided into five genera, including *Iridovirus*, *Chloriridovirus, Ranavirus, Lymphocystisvirus* and *Megalocytivirus* (Chinchar et al., 2005). In recent years, megalocytiviruses have attracted more attention because of their ecological and economic impacts on wild and cultured fishes. A growing number of megalocytiviruses has been found, including infectious spleen and kidney necrosis virus (ISKNV) infecting mandarin fish, *Siniperca chuatsi* (He et al., 2000), red sea bream iridovirus (RSIV) infecting red sea bream, *Pagrus major* (Inouye et al., 1992), sea bass iridovirus (SBIV) infecting sea bass, *Lateolabrax sp*. (Jung et al., 1997), grouper sleep disease iridovirus (GIV) infecting brown-spot grouper, *Epinephelus tauvina* (Chua et al., 1994), rock bream iridovirus (RBIV) infecting rock bream, *Oplegnathus fasciatus* (Jung and Oh, 2000), dwarf gourami iridovirus (DGIV) and African lampeye iridovirus (ALIV) infecting African lampeye, *Aplocheilichthys normani* (Sudthongkong et al., 2001), large yellow croaker iridovirus (LYCIV) infecting large yellow croaker, *Larimichthys crocea* (Chen et al., 2003), and orange-spotted grouper iridovirus (OSGIV) infecting orange-spotted grouper, *Epinephelus coioides* (Lü et al., 2005). Fish infected by megalocystiviruses also include the Malabar grouper, *E. malabaricus* (Danayadol et al., 1996), angelfish, *Pterophyllum scalare*

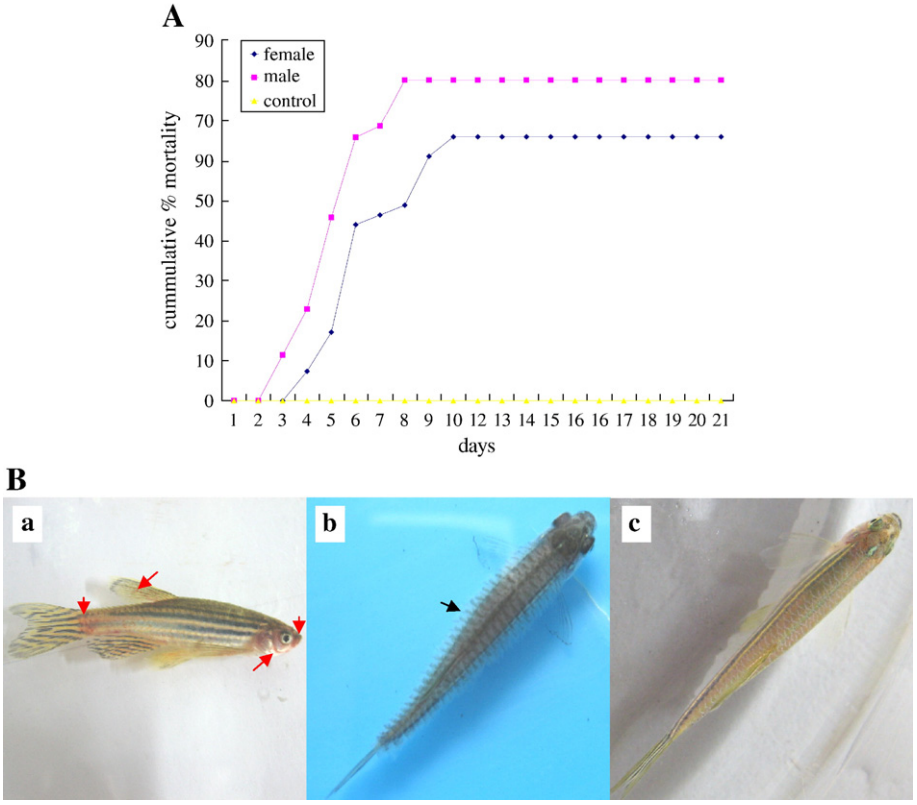

Fig. 1. (A) The cumulative mortalities of zebrafish infected with ISKNV. Adult male or female zebrafish were injected i.p. with 25 μl of ISKNV stocks isolated from diseased mandarin fish and monitored for 21 days. (B) Clinical signs of ISKNV-infected zebrafish. Fish were infected with ISKNV and examined at 4 dpi for signs of viral infection and clinical disease. The diseased fish appear to have heamorrhage in the base of caudal and pectoral fins, abdomen, eyepit, operculum, palate and mandible (red arrows) (a) and scale protrusion (black arrow) (b). The control fish show no clinical signs(c).

(Rodge et al., 1997), grouper, *Epinephelus sp.* (Chou et al., 1998), tilapia, *Oreochromis niloticus* (McGrogan et al., 1998), dwarf gourami, *Colisa lalia* (Sudthongkong et al., 2002), red drum, *Sciaenop socellata* (Weng et al., 2002) and turbot, *Scophthalmus maximus* (Shi et al., 2004).

ISKNV, the causative agent of a disease causing high mortality rates in mandarin fish and severe damage to mandarin fish cultures in China, is regarded as the type species of megalocytiviruses. Wang et al. (2007) have reported that ISKNV-like virus can infect large-mouth bass, *Micropterus salmoides* and more than 50 marine fish. Go et al., (2006) also reported a virus isolated from Murray cod, *Maccullochella peelii peelii*, which has more than 99.9% sequence identity to ISKNV within key viral genes, such as ATPase and the major capsid protein (MCP). Our report is the first to provide evidence that ISKNV can infect the zebrafish (*Danio rerio*, *Cypriniformes*) under experimental conditions.

Like other members of megalocystiviruses, the ISKNV infection of fish is characterized by cell hypertrophy in the spleen, kidney, cranial connective tissue, and endocardium (He et al., 2002). The whole genome of ISKNV has been sequenced (He et al., 2001). However, because of the absence of an applicable animal model for the study of the interactions between the host and the virus, little is known about the functions of ISKNV genes.

In this report we describe the successful infection of adult zebrafish with ISKNV, including infection kinetics, symptoms, histopathology, and the expression of VP23R and MCP genes of the virus. ISKNV can be stably passed and can adapt to replication in zebrafish. Our results provide the first evidence that ISKNV is an effective viral pathogen to zebrafish and will be a valuable platform to study the interactions between the host and virus.

Results

ISKNV infection kinetics and clinical signs

The adult female zebrafish infected with ISKVN filtrates obtained from infected mandarin fish showed a cumulative mortality of 65%. However, the adult male zebrafish were more sensitive to ISKNV infection and showed 80% mortality (Fig. 1A). Mortalities began 3 days post-infection (dpi) and continued through 10 dpi.

Adult zebrafish injected with ISKNV began to show severe clinical symptoms at 3 dpi. The infected fish showed erratic swimming patterns, lingering near the surface of the water, and petechial haemorrhages at the base of the dorsal and pectoral fins, caudal fin, abdomen, palate, and mandible (Fig. 1B-a). Another representative feature was the scale protrusion (Fig. 1B-b). Control fish showed no clinical signs (Fig. 1B-c).

Real-time RT-PCR analyses

The mRNA expression levels of two ISKNV genes, VP23R and MCP were detected in ISKNV-infected zebrafish samples at 12, 14, 36, 48, 72, 96 and 120 hpi by quantitative real-time PCR analysis (Fig. 2). The expression of MCP transcript remained at a basal level before 36 hpi and began to increase at 48 hpi and reached the peak at 96 hpi, which is 136-fold more than that at 12 hpi. The VP23R had periodic expression and reached a peak at 48 and 96 hpi, respectively, which showed 65 and 43-fold increase over that at 12 hpi.

Histopathology of ISKNV infection

An advantage of zebrafish is that the entire animal can be fixed and sectioned in total, which allows inspection of most organs and systems in a single longitudinal section. Fig. 3 showed representative histopathology of the spleens (Fig. 3A and B), kidneys (Fig. 3C and D), and livers (Fig. 3E and F) from the control and ISKNV-infected fish.

Spleens of control fish exhibited distinct marginal zones demarcated by the white pulp (Fig. 3A, black asterisks) and the red pulp (Fig. 3A, white asterisk), which contained a great deal of red blood cells. The brown granules, which were the damaged red blood cells retained by the spleen, were distributed around the vessels (Fig. 3A, black arrow). The swollen spleens of ISKNV-infected zebrafish (Fig. 3B) displayed a large area of necrotic tissue, and the white and the red pulp areas became too blurry to be identified. The amount of red blood cells was reduced and the blood vessels were dilated. The brown regions of the decrepit red blood cells (Fig. 3B, black arrows) became sparse and reduced. Compared with the kidney of healthy fish (Fig. 3C), some of the renal tubules in the kidneys of infected fish (Fig. 3D) displayed a lot of debris from necrotic epithelium and lost the normal shape (Fig. 3D, black asterisks). The interstitial areas between the renal tubules, or glomeruli (Fig. 3D, white asterisk) were also enlarged. In the liver of healthy fish (Fig. 3E), the structure of the tissue was clear and hepatic cells were arranged in a spokewise fashion, surrounding the central vein of the hepatic lobule. The hepatic cord and the hepatic sinusoid were connected to each other and formed a net. We found abundant red blood cells in the liver sinus of healthy fish (Fig. 3E, black arrows), whereas in the liver sinus of ISKNV-

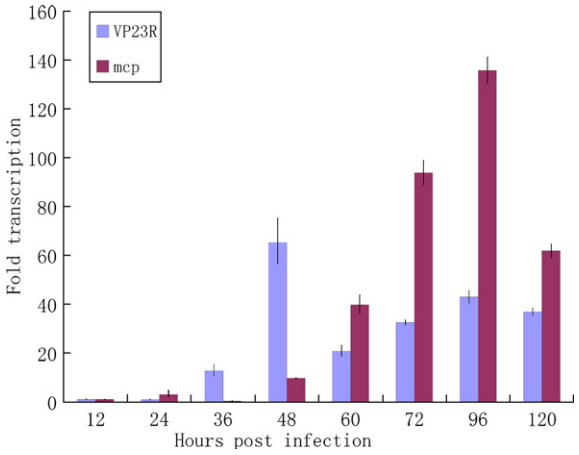

Fig. 2. Quantitative real-time PCR analysis of ISKNV VP23R and MCP mRNA expression in ISKNV-infected zebrafish at 12, 14, 36, 48, 72, 96, and 120 hpi. Transcription values were normalized to zebrafish β-actin and used to calculate the fold values of the transcription of VP23R and MCP over the12 hpi samples.

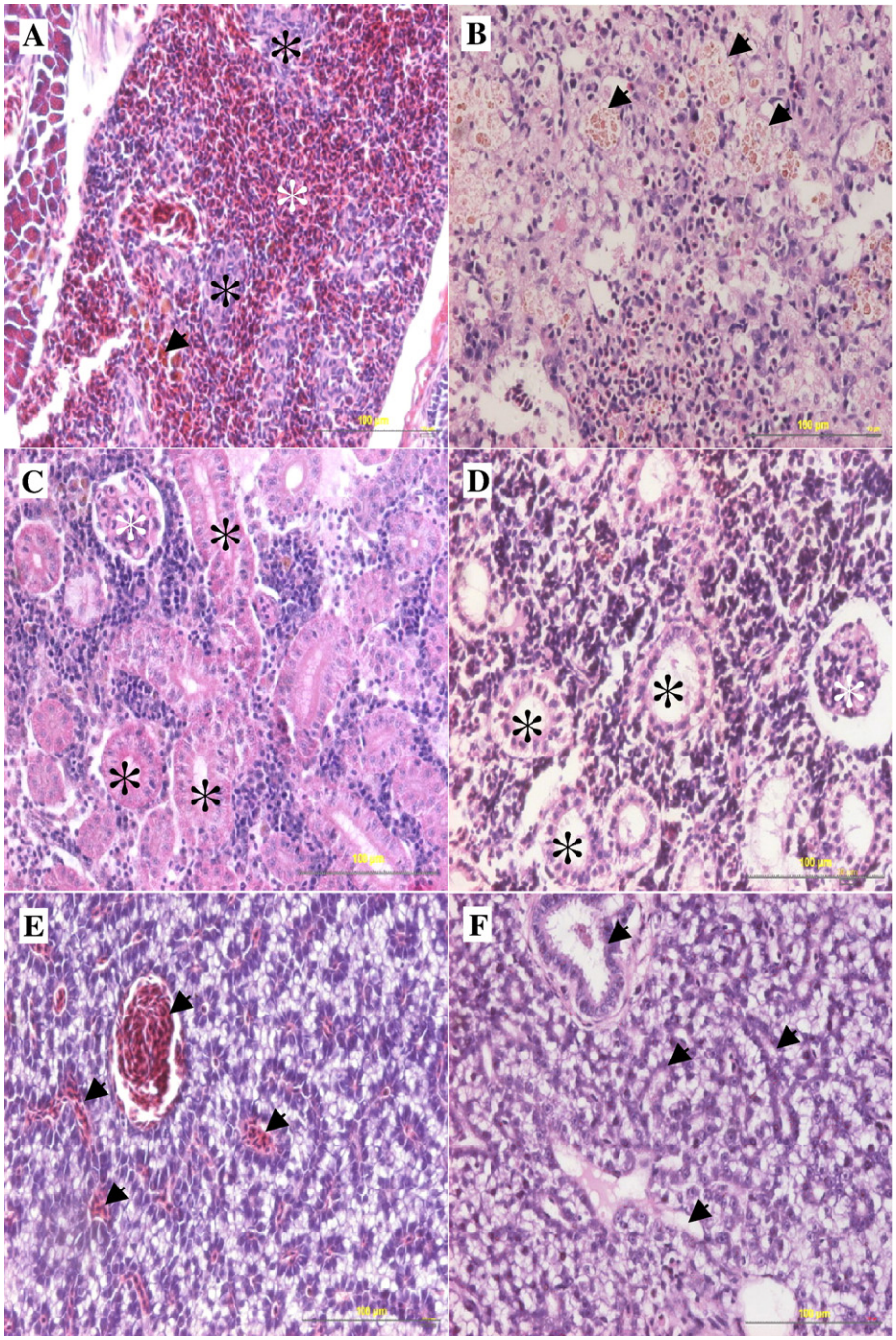

Fig. 3. Histopathology of zebrafish infected with ISKNV (magnification, ×400). Diseased zebrafish were fixed in total and longitudinal sections were prepared and stained with hematoxylin and eosin. (A) Spleen of control fish. Black asterisks indicate white pulp. The white asterisk indicates the red pulp. The black arrow indicates the brown granules. (B) Spleen of infected fish. The white and the red pulp areas are blurry and the brown regions of the decrepit red blood cells (black arrow) become sparse and reduced. (C) Kidney of control fish. Black asterisks indicate renal tubules and the white asterisk indicates the glomeruli. (D) Kidney of infected fish. The interstitial areas of the renal tubules (black asterisks) and glomeruli (white asterisk) are enlarged and in which fewer red blood cells are identified compared with the health fish. (E) Liver of control fish. Abundant red blood cells are found in the liver sinus (black arrow). (F) Liver of infected fish. In the liver sinus (black arrow) the red blood cells are reduced and even non-existent.

infected fish (Fig. 3F black arrows), the red blood cells were reduced or not present. These data indicated that ISKNV infection resulted in similar histopathological changes in zebrafish kidney and spleen as those in mandarin fish (He et al., 2000, 2002).

Immunohistochemistry and immunofluorescence analysis of ISKNV infection

In order to examine the existence and distribution of ISKNV in the infected tissues, the paraformaldehyde-fixed, paraffin-

embedded sections from moribund zebrafish were stained by immunohistochemistry using the polyclonal mouse sera against viral protein VP23R. The VP23R, which is encoded by the ORF23R of ISKNV and specifically localized on the plasma membrane of the ISKNV-infected cells, can be used to mark the infected cells. The presence of hypertrophic cells in tissues was the most characteristic histopathological change of ISKNV-infected fish (He et al., 2002). Specific staining of the plasma membrane with the anti-VP23R antiserum showed that ISKNV-infected hypertrophic cells were present in different organs of moribund zebrafish, including the spleen, kidney, liver, gill, esophagus, gut, and muscle (Fig. 4).

As shown in Fig. 4A, the infected cells in the spleen accumulated in areas showing pathology and were not present in the corresponding normal tissue. In the kidney region of the infected fish, the positive signals existed in the areas between renal tubules (Fig. 4B, black arrowhead) and were mainly detected on the enlarged cells, but not in the epithelia of the renal tubules. In Fig. 4C, the infected cells in liver were fewer and mainly near the vessels. In the gill tissue of infected fish, the infected cells mainly accumulated in the gill plates (Fig. 4D). In the esophagus (Fig. 4E) and gut (Fig. 4F), the infected cells were detected in the stroma. In muscle and skin, the brown signals were present in the intramuscular tissues and subcutaneous tissues (Fig. 4G and H). The nasal cavity of zebrafish was also a habitat of the ISKNV-infected cells, which mainly lay under the olfactory epithelial tissues (Fig. 4I).

The features of ISKNV infection and replication in zebrafish and mandarin fish tissues were compared in double-stained immunofluorescent sections (Fig. 5). The VP23R was visualized in green fluorescence under the stimulation of 488 nm light and MCP was visualized in red fluorescence under 543 nm stimulation. In the convalescent fish at 14 dpi, the immunofluorescent analysis showed that ISKNV existed in musculature, subcutaneous tissues and eyes. The ISKNV displayed different infection patterns in musculature to the connective tissues among the fascicles (Fig. 5A and B). The strong signals of both the VP23R and MCP were detected in the connective tissues

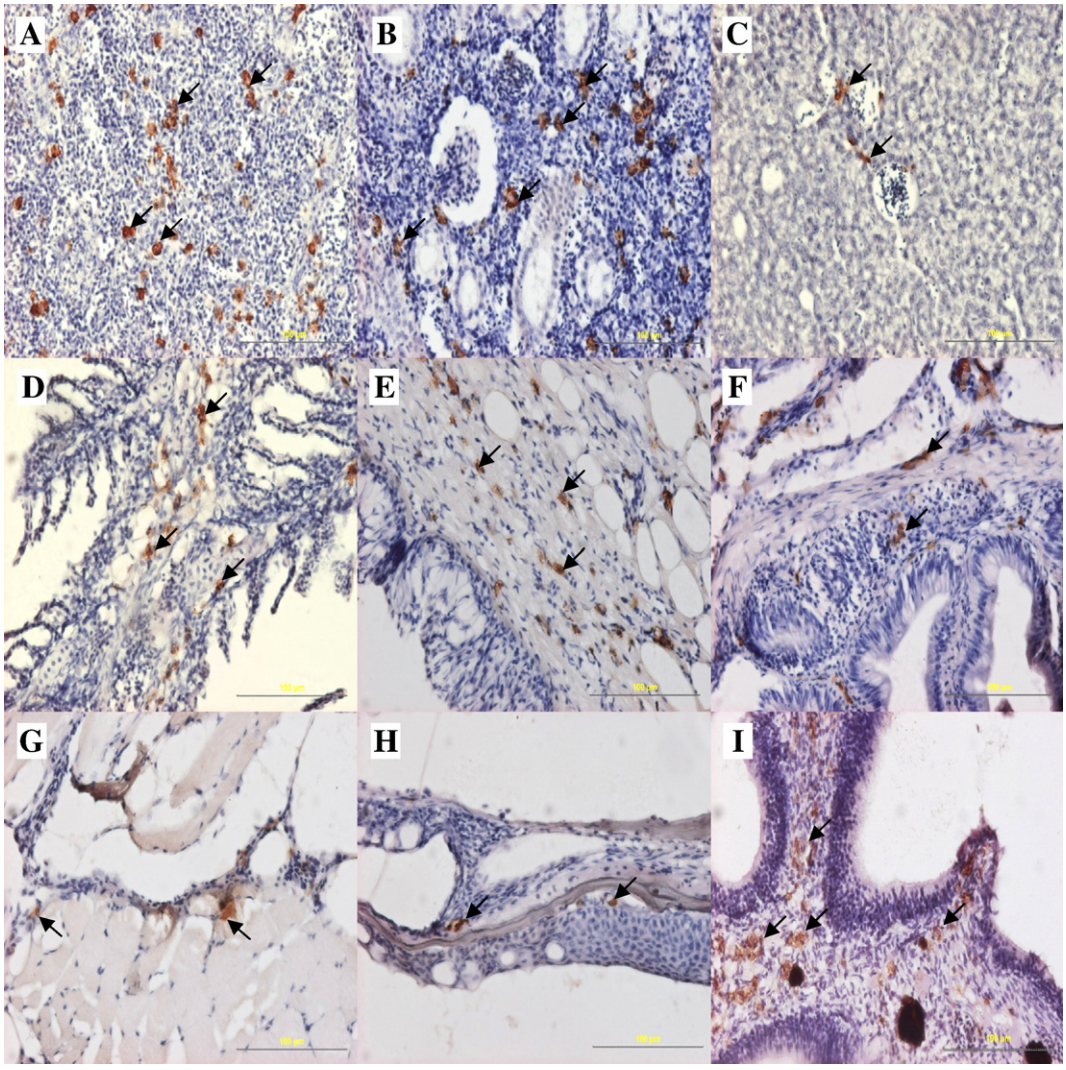

Fig. 4. Immunohistochemical examination of zebrafish infected with ISKNV (magnification, ×400). The zebrafish longitudinal sections were incubated with polyclonal mouse sera against virus protein VP23R and developed by DAB mixture. The ISKNV-infected cells are stained specifically brown on the membrane. (A) spleen; (B) kidney; (C) liver; (D) gill; (E) esophagus; (F) gut; (G) muscle; (H) skin; (I) nasal cavity.

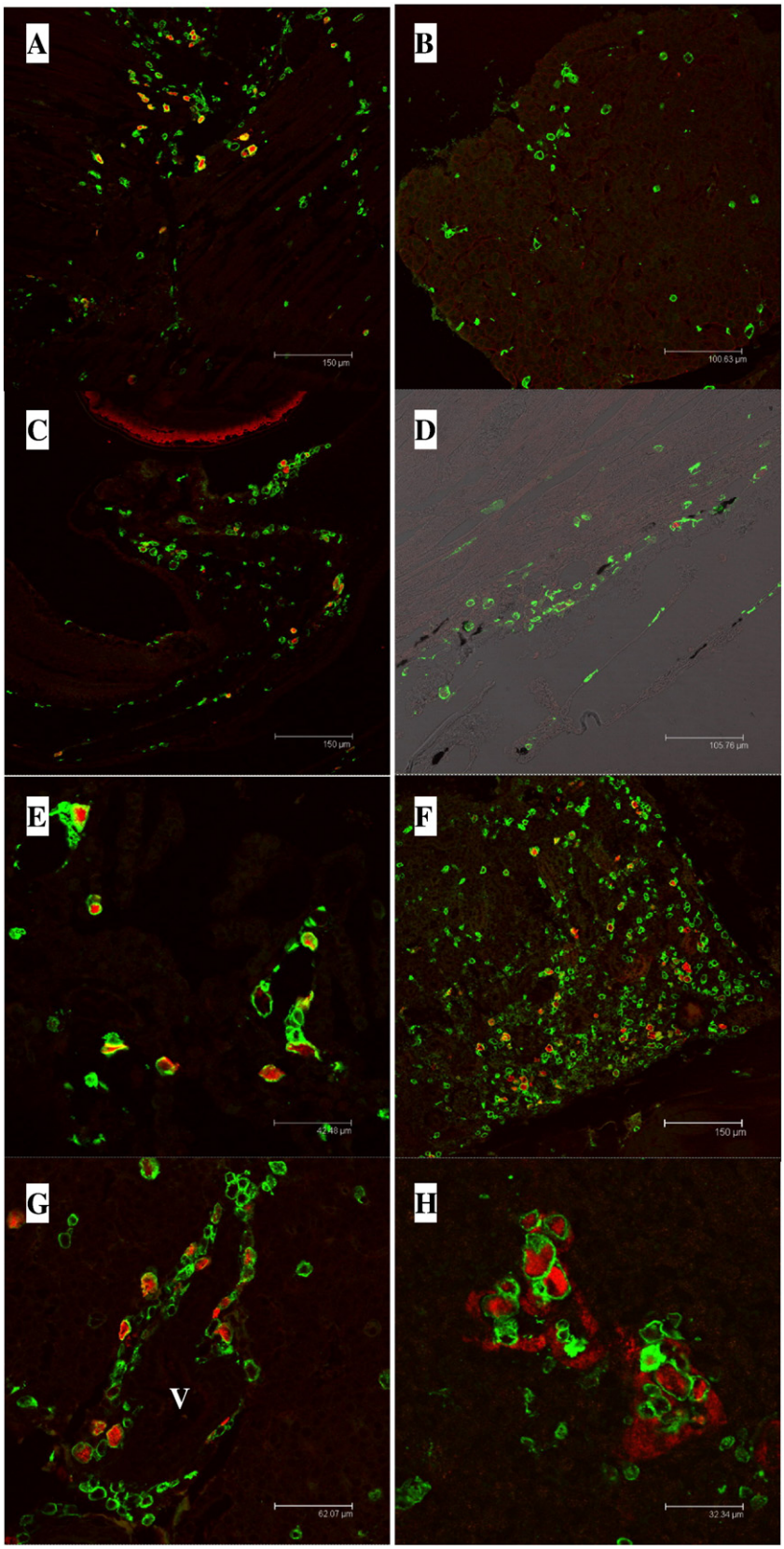

Fig. 5. The double-stained immunofluorescence analysis of tissues from ISKNV-infected zebrafish. The infected cells are labeled with FITC for VP23R (green fluorenscence) and the ISKNV particles are labeled with CY3 for MCP (red fluorenscence). (A) musculature and connective tissues among the fascicles; (B) musculature; (C) eyeball; (D) subcutaneous tissues and cutis; (E) kidney; (F) spleen (V: vessel); (G) spleen of mandarin fish.

among the fascicles (Fig. 5A), whereas the VP23R, but not MCP, was observed in the sporadic infected cells among muscular cells (Fig. 5B). In the eyes of infected fish (Fig. 5C), VP23R signals were detected in the sclera and cornea. This is the first demonstration of ISKNV infecting fish eyes in experimental conditions. Another infection site of ISKNV in zebrafish was subcutaneous tissues, cutis (Fig. 5D), and gills (Fig. 5E).

In zebrafish kidney and spleen tissues (Fig. 5F and G), VP23R signals were found in a certain number of enlarged cells,

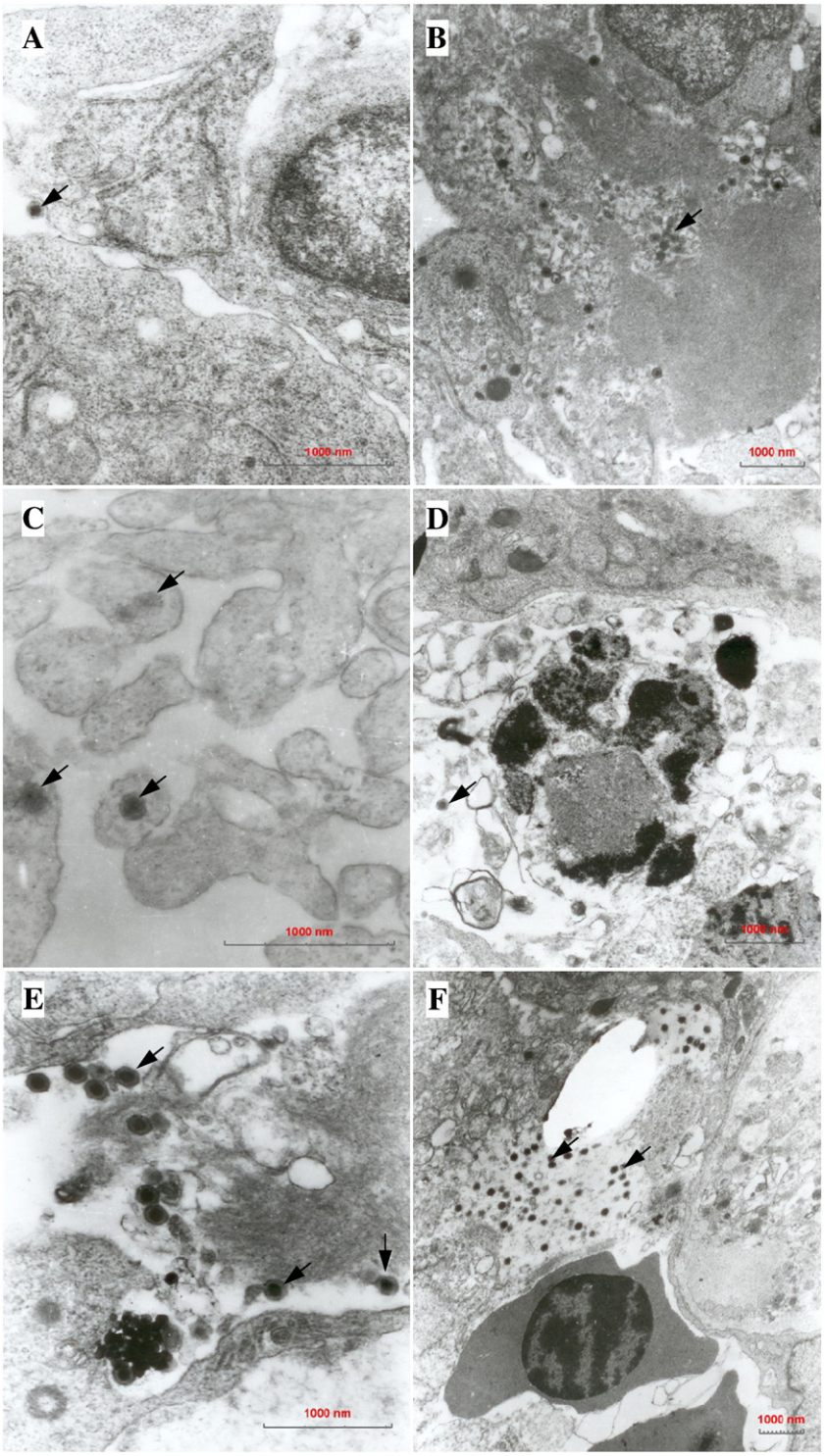

Fig. 6. The electron microscope analysis of spleens from ISKNV-infected zebrafish. (A) A virus particle (black arrow) is attaching and invading a cell (magnification, ×20,000). (B) Virus particles (black arrow) inside cells (magnification, ×10,000). (C) Virus particles (black arrow) inside apoptotic bodies (magnification, ×30,000). (D) A virus particle (black arrow) inside an apoptotic cell (magnification, ×12,000). (E) The releasing virus (magnification, ×25,000). (F) The released virus inside the vessel (magnification, ×8000).

as abundant as that in mandarin fish, indicating that ISKNV could infect zebrafish as effectively as mandarin fish. But the cells in zebrafish containing the MCP of ISKNV were obviously fewer than those in mandarin fish tissues (Fig. 5H). Another remarkable difference was that in the zebrafish tissues, the MCP signals were mainly detected inside the infected cells during the process of ISKNV infection, whereas in mandarin fish, MCP signals had also been detected outside the cells at 5 dpi (Fig. 5H). In fact, we could not find the MCP signals outside the infected cells in a great deal in convalescent fish at 14 dpi or even after the zebrafish host died.

Observation by electron microscope

The spleen sections of ISKNV-infected zebrafish were examined by electron microscope (EM). The size of the ISKNV particles is about 150–200 nm (He et al., 2002). Fig. 6A showed that a virus particle (black arrow) was just attaching an asteroidal cell. Fig. 6B showed a few viral particles of ISKNV scattered in cells or outside cells, but viral particles did not assemble as a crystal lattice in the spleens of zebrafish, which is different from that in mandarin fish (He et al., 2000). Many cells undergoing apoptosis or necrosis were also found in the infected tissues (Fig. 6C and D). We also observed a few mature virus particles releasing from the infected cells and cramming into the vessels (Fig. 6E and F).

ISKNV propagated in zebrafish

ISKNV were passed 10 times in zebrafish and the mortalities of infected zebrafish during each ISKNV passage were shown in Fig. 7A. The mortalities gradually increased and reached a high level at the 10th passage, although the mortalities of the 2nd and 3rd infections were zero. Immunofluorescent analysis showed the obvious releasing of ISKNV from the infected cells in the guts and gills of the 10th-passage-ISKNV challenged zebrafish (Fig. 7B and C).

Discussion

In this report we described the experimental infection of zebrafish with ISKNV and compared the ISKNV pathology in

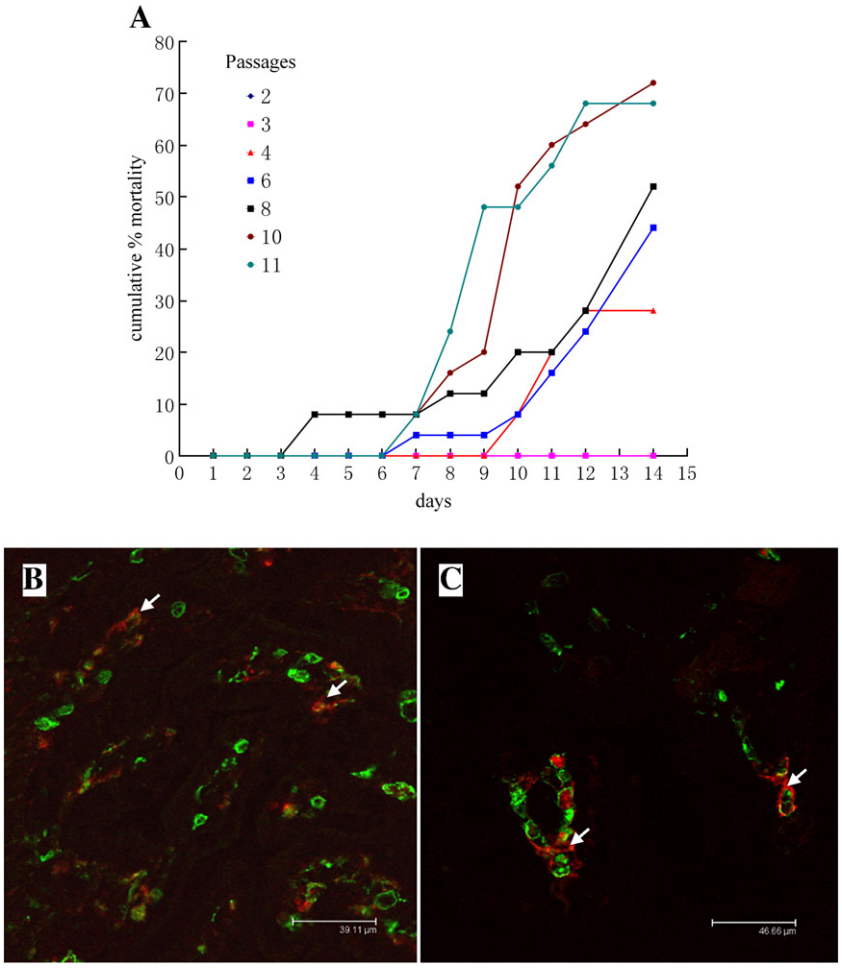

Fig. 7. (A) Comparison of cumulative percent mortalities of zebrafish which is exposed to ISKNV from different passages. Immunofluorenscent detection of the the gut (B) and the gill (C) of the 10th-passage-ISKNV challenged zebrafish. The infected cells were labeled with FITC for VP23R (green fluorenscence) and the releasing ISKNV particles were labeled with CY3 for MCP (red fluorenscence, white arrows).

zebrafish with that in mandarin fish for the first time. The ISKNV i.p. infected zebrafish developed distinct clinical symptoms that resulted in fatal infections. Histological examination of the infected fish showed substantial evidence of viral disease and necrosis. The real-time RT-PCR analysis on the mRNA expression levels of two ISKNV genes, VP23R and MCP further confirmed the virus replication in zebrafish. The use of the mouse anti-VP23R polyclonal antibody allowed detection of ISKNV-infected cells in most organs. Compared with the ISKNV infection in mandarin fish, the MCP signals of ISKNV in zebrafish tissues were fewer, and most of the viral particles were confined inside rather than being released form the infected cells during infection. The EM analysis also confirmed that the virus particles are fewer in the infected zebrafish cells than in mandarin fish cells. The major difference in ISKNV pathology indicates that it replicates somewhat differently in the two fish species.

The symptoms of the infected zebrafish were similar to those of mandarin fish. The natural infection of ISKNV in mandarin fish displays the petechial haemorrhages and the kidney and spleen tumefaction (He et al., 2000). In our experiments, besides haemorrhages, the infected zebrafish displayed scale protrusion, particularly in the last infection stage (Fig. 1B-b), which is similar to the infections of *Aeromonas hydrophila* in carp (Cipriano, 2001) and zebrafish (Pullium et al., 1999). However, the zebrafish infected with ISKNV do not display tail rot, fin rot, and ulcer disease, which were signs of the *Aeromonas hydrophila* infection (Pullium et al., 1999). As the subcutaneous tissue and the cutis are important infection sites of ISKNV, the histopathological changes in these tissues may induce scale protrusion similar to signs of *Aeromonas hydrophila* infection.

Like mandarin fish infected with ISKNV (He et al., 2000, 2002), the prominent features of the infected zebrafish were the hypertrophy of cells in kidney and spleen, and more enlarged cells in spleen than in other organs. Moreover, the infected cells were detected in almost all organs of the infected zebrafish. Considering the challenge method of i.p. injection, the multi-organ infection, especially eye infection, indicated that ISKNV might diffuse through the circulation system, which was supported by a number of virus particles inside the vessels observed by electron microscope (Fig. 6F).

By EM analysis, we have not found the formation of inclusion body-bearing cells (IBCs), which contained the viral assembly sites and was considered as a characteristic of ISKNV infection (He et al., 2000). The enlargement of the ISKNV-infected cells have been considered to be caused by the growth of a unique inclusion body in the IBCs (Chinchar et al., 2005). However, the presence of the enlarged ISKNV-infected cells containing no MCP signals as well as the absence of the IBCs did not support this hypothesis. The enlargement of the ISKNV-infected cells may be due to other factors which need further studies.

As the immunofluorescent examination shown, although the infection rate of ISKNV in zebrafish tissues is as high as that in mandarin fish tissues, the MCP in zebrafish were obviously fewer than those in mandarin fish. In mandarin fish, great amounts of virus were released from the enlarged cells infected by ISKNV at 5 dpi, while the similar phenomena were not found in zebrafish even after death. These data indicate that there may be some unknown mechanisms in zebrafish, which may block the MCP synthesis, the viral particle assembly and release. However, after 10 passages in zebrafish, these blocking mechanisms seem to be attenuated to a certain extent. Because of the limited assembly and release of viral particles in the zebrafish infected with the mandarin fish ISKNV isolate, no death was caused by the 2nd and 3rd passages, but then the mortality began to increase and reached 72% at the 10th passage. We also found that the levels of MCP expression and the assembly of viral particles had increased significantly at the 10th passage and large amounts of viral particles were released, a result very similar to that of mandarin fish, indicating that ISKNV may have adapted to the zebrafish host. The increase of the virulence of ISKNV to zebrafish is likely due to the selective pressures placed upon the virus during replication in different hosts. The specific conditions in a native host often prevent variant virus from replicating and select for those virus particles that will replicate most efficiently in the given host. This selective pressure can affect virulence factors and the overall pathogenicity of the virus significantly. Bruslind and Reno (2000) reported that even one passage of infectious pancreatic necrosis virus (IPNV) in Chinook salmon embryo (CHSE)-214 cells could result in a dramatic change in virulence. This demonstrates that the relationship between selective pressures of the host and virulence is much complex. Therefore, after the passages in zebrafish, the selected virus particles may be accumulated and manifold and may contribute to the increasing mortalities in zebrafish during the passages.

A few zebrafish disease models for viral infection have been documented. LaPatra et al. (2000) found that IHNV and IPNV were able to replicate in zebrafish. Sanders et al. (2003) described a viral pathogen model in adult zebrafish with SVCV. Phelan et al. (2005b) reported that SHRV was an infectious pathogen to both zebrafish adults and embryos. Compared with adult fish, zebrafish embryos are also an important model for bacterial infections because embryos are translucent during the process of development when incubated with 1-pheny-2-thiourea and can be microinjected with some pathogens. The infection with *M. marinum* and *Salmonella typhimurium* was studied in great detail using zebrafish embryos (Prouty et al., 2003; Van der Sar et al., 2003). Compared with mammals, the disadvantage of studying zebrafish is the lack of cell markers and cell lines for experiments (Van der Sar et al., 2004), but the forward genetic screening and the different mutant strains can be used to study the interaction between pathogens and hosts. We report here that ISKNV causes high infection rate and mortalities in zebrafish. The obvious pathological changes have also been demonstrated in the infected tissues of zebrafish. Taken together, the zebrafish can provide a valuable and reliable platform for the studies of ISKNV virulence to the host, which can be used to study the prevention and cure of ISKNV infection, e.g. the development of ISKNV vaccines. More important, since both of the genomes of ISKNV and zebrafish have been sequenced, the zebrafish infected with ISKNV could serve as a good model for research on the immune system of zebrafish as well as the functional genes of ISKNV.

Materials and methods

Zebrafish

Wild type zebrafish were reared and propagated in recirculating systems at 28 °C. The male and female adult fish (3 months old) used in infection experiments were transferred to the isolated flow-through system and allowed to acclimate for 7 days prior to infection.

Virus

ISKNV was isolated from diseased mandarin fish identified in our lab (He et al., 2001) and propagated in mandarin fish. As the source of virus, spleens and kidneys of moribund mandarin fish experimentally infected with ISKNV were homogenized with 1:10 (wt/vol) phosphate-buffered saline (PBS pH 7.4) and centrifuged at 12,000 ×*g* for 10 min at 4 °C. The supernatant was filtered through 0.45 μm membrane and the filtrates were collected and stored at −80 °C. Total DNA of 1 mL of the filtrates was extracted and the level of ISKNV genome equivalents (GE) in the filtrates was determined by absolute quantitative real-time PCR by using the LightCycle 480 System (ROCHE, Germany). Briefly, reactions were performed in a 10 μl volume comprised of 1 ng of total filtrates DNA, 5 μl of 2×SYBRGreen Master Mix (TOYOBO, Japan), 250 nM of the ISKNV MCP specific forward primer (5′-ATCCCCTCCATCACATCCAGCAAG-3′), 250 nM reverse primer (5′-CATgCAggCgTTCCAgAAgTCAAg-3′). The PMD-18T-MCP vector (Takara, Dalian, China) containing one copy of MCP gene was tenfold serial diluted (10^8 to 10^2 copies) as standard in parallel specific real-time PCRs. The copy number of the sample was calculated by the LightCycle software and the level of ISKNV genome equivalents (GE) in the filtrates was determined by conversional calculations. The filtrates were determined containing approximately 2×10^{11} ISKNV GE/mL.

Zebrafish exposure

Adult zebrafish were injected i.p. with 25 μl ISKNV filtrates supplemented with 50 IU/mL penicillin and 50 μg/mL of streptomycin. All control fish were similarly anesthetized and injected with filtrate from spleen and kidney of healthy mandarin fish.

Histology analysis

Adult zebrafish were sampled for histology and placed in 10 mL buffered 10% formalin. The samples were dehydrated by passage through a gradient of ethanol solutions and embedded in paraffin and then longitudinal sections, which contain all organs, were stained with hematoxylin-eosin for microscopic examination.

Electron microscope analysis

Spleens of ISKNV-infected moribund zebrafish at 8–10 dpi were fixed in 2.5% glutaraldehyde in 0.1 M phosphate buffer (pH 7.4). The specimens were then rinsed with 0.1 M phosphate buffer four times and post-fixed in 0.1 M phosphate buffer containing 2.0% osmium tetroxide for 1 h at 4 °C and embedded in Epon's 812 following dehydration. Ultrathin sections were cut and stained with uranyl acetate and lead citrate and examined on a Philips CM10 electron microscopy for the presence of virus particles in hypertrophic cells.

Quantitative real-time PCR

Zebrafish were challenged with ISKNV filtrates as described in Zebrafish exposure and the internal organs of 15 fishes per sample were collected for total RNA extraction at 12, 14, 36, 48, 72, 96, and 120 hour post-infection (hpi). Total RNA of each sample was isolated with TRIzol (Invitrogen, USA) and subjected to DNase I treatment (Promega, USA) according to the manufacturer's protocols. The cDNA was synthesized with SuperScript II RT (Invitrogen, USA) and quantitative real-time PCR was performed using the LightCycle 480 System (ROCHE, Germany). The VP23R specific forward primer (5′-GCCACGCCACCACCTTCTATAAC-3′) together with reverse primer (5′-TGTCGCTTGCCCAAACAATCTTC-3′), which were designed according to the ISKNV ORF023 sequence (accession No. AF37196), and the MCP specific forward primer (5′-ATCCCCTCCATCACATCCAGCAAG-3′) together with reverse primer (5′-CATgCAggCgTTCCAgAAgTCAAg-3′) were used to quantitatively analyze the transcription of VP23 and MCP genes of ISKNV, respectively. Each gene was assayed in triplicate for each sample time point and the zebrafish β-actin, with the forward primer (5′-ATGCCCCTCGTGCTGTTTTC-3′) and the reverse primer (5′-GCCTCATCTCCCACATAGGA-3′), was used to normalize the starting quantity of RNA. Reactions were performed in the LightCycle 480 Systems (ROCHE, Germany) according to the manufacturer's instructions. Reactions were performed in a 10 μl volume comprised of 1 μl of 1:10 cDNA reaction diluted by ddH_2O, 5 μl of 2×SYBRGreen Master Mix (TOYOBO, Japan), and 250 nM concentrations of each primer. The cycling parameters were 95 °C for 2 min to activate the polymerase, followed by 40 cycles of 95 °C for 15 s, 62 °C for 1 min, and 70 °C for 0.1 s, and ended with a 95 °C at 5 °C/s calefactive velocity to make the melt curve. Fluorescence measurements were taken at 70 °C for 0.1 s during each cycle. The copy number for each reaction was calculated by the LightCycle software. Values were normalized to the corresponding β-actin values to determine the relative copy number. The relative copy number was then used to calculate the fold values of the transcription of these two ISKNV genes over the 12 hpi samples.

Immunohistochemistry and immunofluorescence analysis

The ISKNV-infected zebrafish at 8-14 dpi were fixed with 4% paraformaldehyde, paraffin-embedded, and sectioned in total. The longitudinal four-micrometer sections of the samples were deparaffinized in xylene and rehydrated by passage through a gradient of ethanol solutions. Endogenous peroxidase activity was blocked in a 3% hydrogen peroxide solution

and staining of sections was improved by heating for 10 min in citrate buffer pH 6.0 using a microwave. Non-specific binding was blocked by incubation in 10% normal goat serum.

Sections for immunohistochemistry were incubated with mouse anti-VP23R polyclonal mouse sera at 37 °C for 1 h, followed by HRP-conjugated secondary goat anti-mouse antibodies (Jackson ImmunoResearch Laboratories Inc., USA), and developed with DAB for microscopic examination.

Sections for immunofluorescence were incubated with the rabbit-anti-MCP sera prepared in our lab (X.P. Xu, and J.G. He, unpublished data) in a humidified chamber at 37 °C for 1 h. After washing in PBS, the sections were incubated with CY3-conjugated horse anti-rabbit secondary antibody (Sigma, USA) for 30 min. VP23R was then detected using mouse anti-VP23R polyclonal sera, followed by FITC-conjugated secondary goat anti-mouse antibodies (Vector Laboratories, USA). Double-stained sections were observed using a LECA LSM 410 confocal microscope (Germany) at 543 nm for CY3 and 488 nm for FITC, respectively.

Passage of ISKNV in zebrafish

The infection with ISKNV stocks isolated from mandarin fish was treated as the first passage of ISKNV in zebrafish. Upon reisolation from the internal organs including spleen, kidneys, and gut of the moribund ISKNV-infected zebrafish, the viruses were passaged the next 10 times (passages 2–11) in zebrafish.

Acknowledgments

This research was supported by National Natural Science Foundation of China under grant No. 30325035 and U0631008, National Basic Research Program of China under grant No. 2006CB101802, National High Technology Program of China under grant No. 2006AA100309, Guangdong Province Natural Science Foundation under grant No. 20023002, and Science and Technology Bureau of Guangdong Province for Jianguo He and was supported by State High-Tech Research and Development Project (863) of the Ministry of Science and Technology of China (2005AA626011, 2004AA621030, 2003AA626010), Project of National Natural Science Foundation of China (30300264) and Key Project of Guangdong Natural Science Foundation (04205408) and Key Projects of Bureau of Science and Technology of Guangdong Province and Guangzhou City for Anlong Xu.

References

Aballay, A., Yorgey, P., Ausubel, F.M., 2000. *Salmonella typhmurium* proliferates and establishes a persistent infection in the intestine of *Caenorhabditis elegans*. Curr. Biol 10, 1539–1542.

Altmann, S.M., Mellon, M.T., Distel, D.L., Kim, C.H., 2003. Molecular and functional analysis of an interferon gene from the zebrafish, *Danio rerio*. J. Virol 77, 1992–2002.

Altmann, S.M., Mellon, M.T., Johnson, M.C., Paw, B.H., Trede, N.S., Zon, L.I., Kim, C.H., 2004. Cloning and characterization of an Mx gene and its corresponding promoter from the zebrafish, *Danio rerio*. Dev. Comp. Immunol 28, 295–306.

Brenot, A., King, K.Y., Janowiak, B., Griffith, O., Caparon, M.G., 2004. Contribution of glutathione peroxidase to the virulence of *Streptococcus pyogenes*. Infect. Immun 72, 408–413.

Bruslind, L.D., Reno, P.W., 2000. Virulence comparison of three Buhl-subtype isolates of infectious pancreatic necrosis virus in brook trout fry. J. Aquat. Anim. Health 12, 301–315.

Chen, X.H., Lin, K.B., Wang, X.W., 2003. Outbreaks of an iridovirus disease in maricultured large yellow croaker, *Larimichthys crocea* (Richardson), in China. J. Fish Dis 26, 615–619.

Chinchar, V.G., Essbauer, S., He, J.G., Hyatt, A., Miyazaki, T., Seligy, V., Williams, T., 2005. Part II the double stranded DNA viruses, family Iridoviridae. In: Fauquet, C.M., Mayo, M.A., Maniloff, J., Desselberger, U., Ball, L.A. (Eds.), Virus Taxonomy, VIIIth Report of the International Committee on Taxonomy of Viruses. Elsevier/Academic Press, London, pp. 145–162.

Chou, H.Y., Hsu, C.C., Peng, T.Y., 1998. Isolation and characterization of a pathogenic iridovirus from cultured grouper (*Epinephelus sp.*) in Taiwan. Fish Pathol 33, 201–206.

Chua, H.C., Ng, M.L., Woo, J.J., Wee, J.Y., 1994. Investigation of outbreaks of a novel disease, "Sleepy Grouper Disease", affecting the brown-spotted grouper, *Epinephelus tauvina Forskal*. J. Fish Dis. 17, 417–427.

Cipriano, R.L., 2001. *Aeromonas hydrophila* and motile Aereomonad Septicemias of fish. Fish and Disease Leaflet 68. http://www.lsc.usgs.gov/FHB/leaflets/FHB68.pdf.

Danayadol, Y., Direkbusarakom, S., Boonyaratpalin, S., Miyazaki, T., Miyata, M., 1996. An outbreak of iridovirus-like infection in brownspotted grouper (*Epinephelus malabaracus*) cultured in Thailand. AAHRI Newslett 5, 6.

Danilova, N., Bussmann, J., Jekosch, K., Steiner, L.A., 2005. The immunoglobulin heavy-chain locus in zebrafish: identification and expression of a previously unknown isotype, immunoglobulin Z. Nat. Immunol 6, 295–302.

Darai, G., Anders, K., Koch, H.G., Delius, H., Gelderblom, H., Samalecos, C., Flugel, R.M., 1983. Analysis of the genome of fish lymphocystis disease virus isolated directly from epidermal tumours of pleuronectes. Virology 126, 466–479.

Darai, G., Deliu, H., Clark, J., Apfel, H., Schnitzler, P., Flugel, R.M., 1985. Molecular cloning and physical mapping of the genome of fish lymphocystis disease virus. Virology 146, 292–301.

Davis, J.M., Clay, H., Lewis, J.L., Ghori, N., Herbomel, P., Ramakrishnan, L., 2002. Real-time visualization of mycobacterium macrophage interactions leading to initiation of granuloma formation in zebrafish embryos. Immunity 17, 693–702.

Delius, H., Darai, G., Flugel, R.M., 1984. DNA analysis of insect iridescent virus 6: evidence for circular permutation and terminal redundancy. J. Virol 49, 609–614.

Go, J., Lancaster, M., Deece, K., Dhungyel, O., Whittington, R., 2006. The molecular epidemiology of iridovirus in Murray cod (*Maccullochella peelii peelii*) and dwarf gourami (*Colisa lalia*) from distant biogeographical regions suggests a link between trade in ornamental fish and emerging iridoviral diseases. Mol. Cell Probes 20, 212–222.

Gunimaladevi, I., Savan, R., Sakai, M., 2006. Identification, cloning and characterization of interleukin-17 and its family from zebrafish. Fish Shellfish Immunol 21, 393–403.

He, J.G., Deng, M., Weng, S.P., Li, Z., Zhou, S.Y., Long, Q.X., Wang, X.Z., Chan, S.M., 2001. Complete genome analysis of the mandarin fish infectious spleen and kidney necrosis iridovirus. Virology 291, 126–139.

He, J.G., Zeng, K., Weng, S.P., Chan, S.M., 2000. Systemic disease caused by an iridovirus-like agent in cultured mandarinfish, *Sinipercachuatsi* (Basil-lewsky), in China. J. Fish Dis 23, 219–222.

He, J.G., Zeng, K., Weng, S.P., Chan, S.M., 2002. Experimental transmission, pathogenicity and physical–chemical properties of infectious spleen and kidney necrosis virus (ISKNV). Aquaculture 204, 11–24.

Herbomel, P., Thisse, B., Thisse, C., 1999. Ontogeny and behaviour of early macrophages in the zebrafish embryo. Development 126, 3735–3745.

Igawa, D., Sakai, M., Savan, R., 2006. An unexpected discovery of two interferon gamma-like genes along with interleukin (IL)-22 and -26 from teleost: IL-22 and -26 genes have been described for the first time outside mammals. Mol. Immunol 43, 999–1009.

Inouye, K., Yamano, K., Maeno, Y., Nakajima, K., Matsuoka, M., Wada, Y., Sorimachi, M., 1992. Iridovirus infection of cultured red sea bream, *Pagrus major*. Fish Pathol 27, 19–27.

Jault, C., Pichon, L., Chluba, J., 2004. Toll-like receptor gene family and TIR-domain adapters in *Danio rerio*. Mol. Immunol 40, 759–771.

Jung, S., Miyazaki, T., Miyata, M., Danayadol, Y., Tanaka, S., 1997. Pathogenicity of iridovirus from Japan and Thailand for the red sea bream *Pagrus major* in Japan, and histopathology of experimentally infected fish. Fisheries Sci 63, 735–740.

Jung, S.J., Oh, M.J., 2000. Iridovirus-like infection associated with high mortalities of striped beakperch, *Oplegnathus fasciatus* (Temmink et Schlegel), in southern coastal areas of the Korean peninsula. J. Fish Dis. 23, 223–226.

LaPatra, S.E., Barone, L., Jones, G.R., Zon, L.I., 2000. Effects of infectious hematopoietic necrosis virus and infectious pancreatic necrosis virus infection on hematopoietic precursors of the zebrafish. Blood Cells Mol. Dis 26, 445–452.

Lü, L., Zhou, S.Y., Chen, C., Weng, S.P., Chan, S.M., He, J.G., 2005. Complete genome sequence analysis of an iridovirus isolated from the orange-spotted grouper, *Epinephelus coioides*. Virology 339, 81–100.

McGrogan, D.G., Ostland, V.E., Byrne, P.J., Ferguson, H.W., 1998. Systemic disease involving an iridovirus-like agent in cultured tilapia, *Oreochromis niloticus L*. J. Fish Dis 21, 149–152.

Meijer, A.H., Gabby Krens, S.F., Medina Rodriguez, I.A., He, S., Bitter, W., Ewa Snaar-Jagalska, B., Spaink, H.P., 2004. Expression analysis of the Toll-like receptor and TIR domain adaptor families of zebrafish. Mol. Immunol 40, 773–783.

Menudier, A., Rougier, F.P., Bosgiraud, C., 1996. Comparative virulence between different strains of *Listeria* in zebrafish (*Brachydanio rerio*) and mice. Pathol. Biol 44, 783–789.

Neely, M.N., Pfeifer, J.D., Caparon, M., 2002. Streptococcus-zebrafish model of bacterial pathogenesis. Infect. Immun 70, 3904–3914.

Novoa, B., Romero, A., Mulero, V., Rodriguez, I., Fernandez, I., Figueras, A., 2006. Zebrafish (*Danio rerio*) as a model for the study of vaccination against viral haemorrhagic septicemia virus (VHSV). Vaccine 24, 5806–5816.

O'Toole, R., Von Hofsten, J., Rosqvist, R., Olsson, P.E., Wolf-Watz, H., 2004. Visualisation of zebrafish infection by GFP-labelled *Vibrio anguillarum*. Microb. Pathog 37, 41–46.

Phelan, P.E., Mellon, M.T., Kim, C.H., 2005a. Functional characterization of full-length TLR3, IRAK-4, and TRAF6 in zebrafish (*Danio rerio*). Mol. Immunol 42, 1057–1071.

Phelan, P., Pressley, M.E., Witten, P.E., Mellon, M.T., Blake, S., Kim, C.H., 2005b. Characterization of *Snakehead rhabdovirus* infection in zebrafish (*Danio rerio*). J. Virol 79, 1842–1852.

Prouty, M.G., Correa, N.E., Barker, L.P., Jagadeeswaran, P., Klose, K.E., 2003. Zebrafish-*Mycobacterium marinum* model for mycobacterial pathogenesis. FEMS Microbiol. Lett 225, 177–182.

Pukatzki, S., Kessin, R.H., Mekalanos, J.J., 2002. The humanpathogen *Pseudomonas aeruginosa* utilizes conserved virulence pathways to infect the social amoeba *Dictyostelium discoideum*. Proc. Natl. Acad. Sci 99, 3159–3164.

Pullium, J.K., Dillehay, D.L., Webb, S., 1999. High mortality in zebrafish (*Danio rerio*). Contemp. Top Lab Anim Sci 38, 80–83.

Rodge, H.D., Kobs, M., Macartney, A., Frerichs, G.N., 1997. Systemic iridovirus infection in freshwater angelfish, *Pterophyllum scalare* (Lichtenstein). J. Fish Dis 20, 69–72.

Sanders, G.E., Batts, W.N., Winton, J.R., 2003. Susceptibility of zebrafish (*Danio rerio*) to a model pathogen, spring viremia of carp virus. Comp. Med 53, 514–521.

Shi, C.Y., Wang, Y.G., Yang, S.L., Huang, J., Wang, Q.Y., 2004. The first report of an iridovirus-like gent infection in farmed turbot, *Scophthalmus maximus*, in China. Aquaculture 236, 11–25.

Sudthongkong, C., Miyata, M., Miyazaki, T., 2001. Iridovirus disease in two ornamental tropical freshwater fishes: African lampeye and dwarf gourami. Dis. Aquat. Org 48, 163–173.

Sudthongkong, C., Miyata, M., Miyazaki, T., 2002. Viral DNA sequence of genes encoding the ATPase and the major capsid protein of tropical iridovirus isolates which are pathogenic to fishes in Japan, South China Sea and Southeast Asian countries. Arch. Virol 147, 2089–2109.

Suttle, C.A., 2005. Viruses in the sea. Nature 437, 356–361.

Tidona, C.A., Darai, G., 1997. The complete DNA sequence of lymphocystis disease virus. Virology 230, 207–216.

Trede, N.S., Langenau, D.M., Traver, D., Look, A.T., Zon, L.I., 2004. Use of zebrafish to understand immunity. Immunity 20, 367–379.

Van der Sar, A.M., Appelmelk, B.J., Vandenbroucke-Grauls, C.M.J.E., Bitter, W., 2004. A star with stripes: zebrafish as an infection model. Trends Microbiol 12, 451–457.

Van der Sar, A.M., Musters, R.J., van Eeden, F.J., Appelmelk, B.J., Vandenbroucke-Grauls, C.M., Bitter, W., 2003. Zebrafish embryos as a model host for the real time analysis of *Salmonella typhimurium* infections. Cell. Microbiol 5, 601–611.

Wang, Y.Q., Lu, L., Weng, S.P., Huang, J.N., Chan, S.M., He, J.G., 2007. Molecular epidemiology and phylogenetic analysis of a marine fish infectious spleen and kidney necrosis virus-like (ISKNV-like) virus. Arch. Virol 152, 763–773.

Weng, S.P., Wang, Y.Q., He, J.G., Deng, M., Lü, L., Guan, H., Liu, J., Chan, Y.J., 2002. Outbreaks of an iridovirus in red drum, *Sciaenops ocellata* (L.), cultured in southern China. J. Fish Dis 25, 681–685.

Williams, T., 1996. The iridoviruses. Adv. Virus Res 46, 345–412.

Willis, D.B., Granoff, A., 1980. Frog virus 3 DNA is heavily methylated at CpG sequences. Virology 107, 250–257.

Yoder, J.A., Litman, R.T., Mueller, M.G., 2004. Resolution of the novel immune-type receptor gene cluster in zebrafish. Proc. Natl. Acad. Sci. U. S. A 44, 15706–15711.

Zhang, D.C., Shao, Y.Q., Huang, Y.Q., Jiang, S.G., 2005. Cloning, characterization and expression analysis of interleukin-10 from the zebrafish (*Danio rerion*). J. Biochem. Mol. Biol 38, 571–576.